$Er_7Ni_2Te_2$: The Most Rare-Earth Metal-Rich Ternary Chalcogenide

Fanqin Meng and Timothy Hughbanks*

Department of Chemistry, Texas A&M University, P.O. Box 30012, College Station, Texas 77842-3012

Received January 3, 2001

Synthetic exploration of metal-rich chalcogenides of group IV and V early transition metals incorporating the Brewer−Wengert concept of polar intermetallic bonding[1] has provided a great variety of new chemistry. Recent extension of this research to the electron-poorer rare-earth metal systems has produced $Sc_5Ni_2Te_2$,[2] Sc_6MTe_2 (M = Mn, Fe, Co, Ni, Pd),[3] Dy_6MTe_2 (M = Fe, Co, Ni),[4] $Y_5M_2Te_2$ (M = Fe, Co, Ni),[5] $R_5M_2Te_2$ (R = Gd, Dy, Er, M = Co, Ni),[6] and R_6MTe_2 (R = Gd, Er, M = Co, Ni, Ru).[7] The new compound $Er_7Ni_2Te_2$ reported here represents the most metal-rich of the ternary rare-earth chalcogenides. Rare-earth elements and many of their compounds exhibit a range of fascinating physical properties originating from localized 4f electrons. The magnetic properties of rare-earth systems have received extensive attention due to their technological importance and scientific challenges. Magnetic properties of the title compound were measured and analyzed in this report.

Er_3Ni and $NiTe_2$ were prepared by direct reaction of stoichiometric elements (Er foil, Ames Lab 99.99%; Te powder, Alfa 99.99%; Ni powder, Alfa 99.95%) via arc melting and solid-state reactions in sealed silica tubes, respectively. Appropriate ratios of Er, Er_3Ni, and $NiTe_2$ were wrapped in molybdenum foil, which was sealed in flame-baked silica tube under vacuum. This vessel was heated between 800 and 1100 °C for 7 days; the product contained $Er_7Ni_2Te_2$ in 80−90% yield, with ErTe as the only other observable phase in a Guinier powder diffraction pattern. The target compound is also accessible in quantitative yield by heating the above vessel at 850 °C for 4 weeks or by using molybdenum foil within a niobium tube as the reaction container. Black rods suitable for single-crystal X-ray studies were obtained, and the compound was found to adopt a new structure type with space group *Imm*2 (No. 44). Synthesis of the cobalt analogue afforded an isostructural compound in high yield.

The structure[8] of $Er_7Ni_2Te_2$, projected along the [010] direction, is shown in Figure 1. The basic structural unit is a distorted, Ni-centered, tricapped trigonal prism (TTP) of Er that is fused with like prisms by sharing the Er_3 triangular bases to form an infinite $[(Er_3Er_{3/2}Er_{3/2})Ni]_\infty$ chain that propagates along the *b* axis. These infinite chains are condensed to form corrugated layers across the *bc* plane by sharing Er zigzag chains, which are composed of capping Er atoms on one TTP and inner Er on the adjacent TTP (**1**). Finally, vertex condensation forms links between individual layers that result in the overall 3-D structure (**2**). Tellurium atoms reside between the metal−metal bonded layers, on *bc* planes.

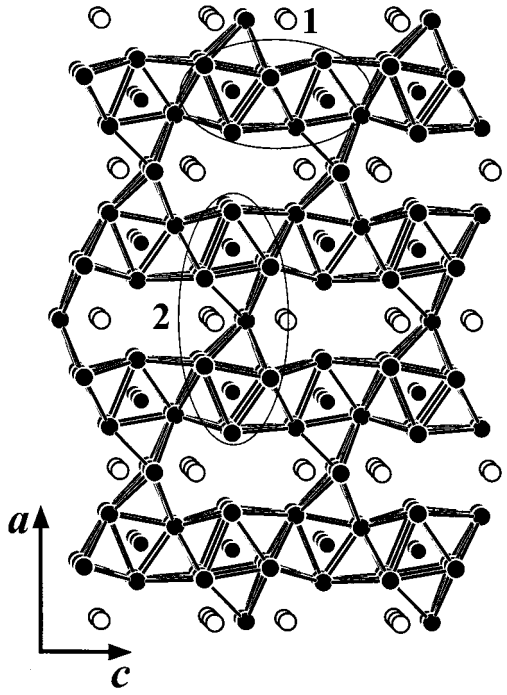

Figure 1. Approximate [010] projection of the $Er_7Ni_2Te_2$ structure. Er and Ni atoms are shown as dark circles with and without bonds, respectively. Te are open circles. Er−Te and Er−Ni bonds are not shown for clarity. Circled regions **1** and **2** are depicted below.

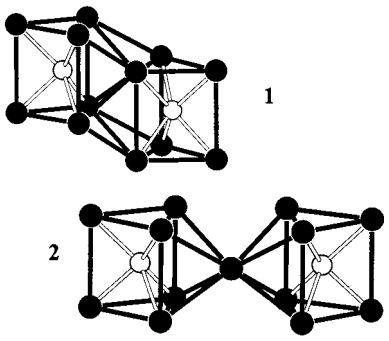

This work is placed in context by examining the structural relationship between $Er_7Ni_2Te_2$ and three other structures: Zr_6CoAl_2-type (e.g., Zr_6MTe_2,[9] Sc_6MTe_2,[3] Gd_6MTe_2[7]), Hf_5FeTe_3,[10] and Zr_3Fe.[11] All four structures can be constructed using centered TTPs as fundamental building blocks, but following different

* To whom correspondence should be addressed.

(1) Brewer, L.; Wengart, P. R. *Metall. Trans.* **1973**, *4*, 2674.
(2) Maggard, P. A.; Corbett, J. D. *Inorg. Chem.* **1999**, *38*, 1945−50.
(3) Maggard, P. A.; Corbett, J. D. *Inorg. Chem.* **2000**, *39*, 4143−6.
(4) Bestaoui, N.; Herle, P. S.; Corbett, J. D. *J. Solid State Chem.* **2000**, *155*, 9−14.
(5) Maggard, P. A.; Corbett, J. D. *J. Am. Chem. Soc.* **2000**, *122*, 10740−1.
(6) Meng, F.; Hughbanks, T. Unpublished results.
(7) Meng, F.; Hughbanks, T. Unpublished results.
(8) Single-crystal (0.27 × 0.03 × 0.02 mm) data of $Er_7Ni_2Te_2$ were collected at 110 K on a Bruker SMART CCD diffractometer, which indicated a body-centered orthorhombic cell. A total of 1823 reflections ($5° < 2\theta \leq 58°$) were collected, of which 770 were unique ($R_{int} = 0.0995$). The structure was refined in the orthorhombic space group *Imm*2 (No. 44, $Z = 2$), lattice parameters $a = 15.345(3)$ Å, $b = 3.8377(8)$ Å, $c = 9.438(2)$ Å. Direct methods were used to locate all the atoms, and anisotropic refinement converged to R1 = 0.0424, wR2 = 0.0994.

(9) Wang, C.; Hughbanks, T. *Inorg. Chem.* **1996**, *35*, 6987−94.
(10) Abdon, R. L.; Hughbanks, T. *J. Am. Chem. Soc.* **1995**, *117*, 10035−40.
(11) Malakhova, T. O.; Alekseyeva, Z. M. *J. Less-Common Met.* **1981**, *81*, 293−300.

10.1021/ic010009h CCC: $20.00
Published on Web 04/27/2001

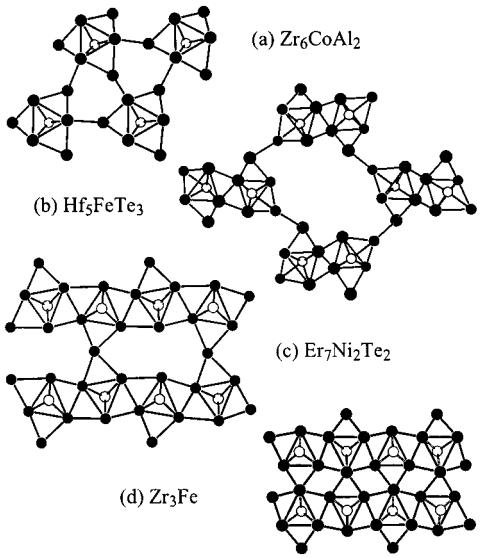

Figure 2. Arrangements of TTPs into (a) single chains in the Zr_6CoAl_2 structure, (b) double chains in the Hf_5FeTe_3 structure, (c) layers in the $Er_7Ni_2Te_2$ structure, and (d) a 3-D network in the Zr_3Fe structure. Early transition metals are shown as larger circles, and late transition metals are smaller. Some metal−metal bonds are omitted for clarity.

condensation schemes (Figure 2). In the Zr_6CoAl_2-type structure, bonding between the capping and apical atoms of adjacent TTPs interconnects single TTP chains. In the Hf_5FeTe_3 structure, double chains are formed by edge condensation of single chains, and the so-formed double chains are stitched together into a 3-D network by forming longer bonds between the capping atoms not involved in condensation. As described previously, formation of condensed intermetallic layers becomes characteristic in the $Er_7Ni_2Te_2$ structure. Successive layers are shifted relative to one another along the *c* direction and are linked together by sharing capping atoms such that Te atoms are accommodated at two chemically inequivalent sites between the layers. A similar but more symmetrical layer architecture is found in the structure of Zr_3Fe, which in turn is closely related to hexagonal-close-packing metals. Adjacent layers in the Zr_3Fe structure stack vertically in Figure 2d, sharing one Zr atom in every TTP unit. This 3-D network is even more condensed due to the formation of extensive Zr−Zr bonds between the layers.

Electronic band structure calculations for $Er_7Ni_2Te_2$ were performed with the extended Hückel method[12] using the YAeHMOP package.[13] The Fermi level intersects a prominent conduction band having mainly Er 5d and 6s character, indicating that this material is a metallic conductor, as expected. The majority of the Ni 3d states lie at lower energies, consistent with significant polarity of the Er−Ni bonds. COOP (crystal orbital overlap population) calculations indicate Er−Ni that bonding is optimized in that the Fermi level is at the crossover of the Er−Ni bonding and antibonding states. Er−Er bonding appears to impose weaker constraints on the structure because shorter Er−Er bonds do not always possess higher overlap populations. This treatment agrees well with the previous structural description. The persistence of the late-transition-metal-centered TTP unit in various intermetallic compounds is a result of the strong heterometallic bonding. With increasing late-transition-metal contents, TTP units link together to form single chains, then double chains, then layers or 3-D networks by angular distortion of the bonds between the early transition or rare-earth metals.

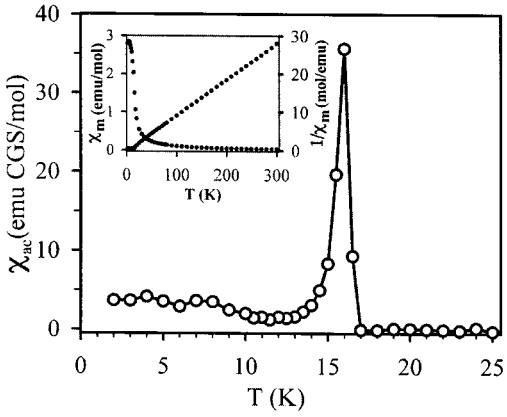

Figure 3. The ac susceptibility of polycrystalline $Er_7Ni_2Te_2$. Inset: temperature dependence of χ_m and χ_m^{-1}.

Magnetic measurements on a polycrystalline sample (12.74 mg) were carried out with the use of a Quantum Design (model MPMS-5) SQUID magnetometer. Temperature-dependent susceptibility data were collected from 2 to 300 K at a field of 1000 G. The magnetic susceptibility data (χ) were corrected for the paramagnetic impurity (ErTe) contribution,[12] for sample holder contribution, and for the intrinsic diamagnetic contribution;[15] temperature independent paramagnetism was found to be negligible within the experimental error.

Between 100 and 300 K, χ is fit with the Curie−Weiss expression, $\chi = C/(T - \theta)$; a χ^{-1} versus T plot (Figure 3, inset) gave $C = 10.6 \pm 0.2$ and $\theta = 4.1(4)$ K. The effective moment, $\mu_{eff} \simeq \sqrt{8C}$, was 9.21 ± 0.09 μ_B, to be compared with 9.58 μ_B calculated for free Er^{3+} ($^4I_{15/2}$). Reported μ_{eff} values for Er_2Te_3,[14] ErTe,[14] and Er metal[16] are 9.50 ± 0.14, 9.35 ± 0.14, and 8.98 ± 0.18 μ_B, respectively. The more numerous the Er−Er bonds, the lower the observed μ_{eff}. The effective moment for $Er_7Ni_2Te_2$ is at the expected place in this series.

An ac susceptibility measurement demonstrates an ordering transition at $T_C = 16.5$ K (Figure 3). Ordering in $Er_7Ni_2Te_2$ and in Er metal ($T_C = 18$ K) can be attributed to the RKKY exchange interaction between the Er moments, which is indirect in nature and is mediated through itinerant conduction electrons.[17−19] This is the first metal-rich rare-earth chalcogenide for which a magnetic transition has been observed.

Acknowledgment. This work was supported by Texas Advanced Technology Program (Grant 010366-00386-1997). The CCD equipped diffractometer and SQUID magnetometer were acquired with NSF grants (CHE9807975 and CHE9974899). We thank Dr. Xiaobing Xie and Dr. Jiang-gao Mao are acknowledged for help with crystal structure refinement, and Mr. Bradley Smucker for help with the magnetic measurements.

Supporting Information Available: X-ray crystallographic files for $Er_7Ni_2Te_2$ in CIF format. This material is available free of charge via the Internet at http://pubs.acs.org.

IC010009H

(12) Hoffmann, R. *J. Chem. Phys.* **1963**, *39*, 1397−412.
(13) Landrum, G. A. *YAeHMOP: Yet Another Extended Hückel Molecular Orbital Package.* YAeHMOP is available on the web: http://overlap.chem.cornell.edu:8080/yaehmop.html.
(14) Hoggins, J.; Steinfink, H. *Inorg. Chem.* **1968**, *7*, 826−8.
(15) Boudreaux, E. A., Mulay, L. N., Eds. *Theory and Applications of Molecular Paramagnetism*; John Wiley & Sons: New York, 1976.
(16) McEwen, K. A. In *Magnetic and transport properties of the rare earths*; Gschneidner, K. A., Eyring, L. R., Eds.; *Handbook on the Physics and Chemistry of Rare Earths*, Vol.1; North-Holland: Amsterdam, New York, Oxford, 1978; p 427.
(17) Ruderman, M. A.; Kittel, C. *Phys. Rev.* **1954**, *96*, 99.
(18) Kasuya, T. *Prog. Theor. Phys. (Kyoto)* **1956**, *16*, 45.
(19) Yosida, K. *Phys. Rev.* **1957**, *106*, 893.